

A high-gain optical injection amplification system for coherent fiber links

Ru Yuan(袁茹), Xiang Zhang(张翔), Qian Zhou(周茜), Qi Zang(臧琦), Bo-Lin Zhang(张林波), Yi-Ting Liu(刘依婷), Dan Wang(王丹), Jie Liu(刘杰), Yu-Can Zhang(张钰灿), Yu-Fang Lei(雷语芳), Tao Liu(刘涛), Rui-Fang Dong(董瑞芳), and Shou-Gang Zhang(张首刚)

Citation: Chin. Phys. B, 2026, 35 (**4**): 044209. DOI: 10.1088/1674-1056/ae111a
http://cpb.iphy.ac.cn; http://iopscience.iop.org/cpb

What follows is a list of articles you may be interested in

Full stabilization of eight-channel Yb-fiber coherent beam combining system delivering 1.18-kW, 1.18-mJ, 270-fs pulses

Zhuo Shi(史卓), Zhi-Hang Du(杜志航), Cheng-Bin Liang(梁成斌), Hong-Xiang Chang(常洪祥), Zi-Kai Dong(董自凯), Hong-Yu Guo(郭鸿宇), Can Li(李灿), Pu Zhou(周朴), Zhi-Yi Wei(魏志义), and Guo-Qing Chang(常国庆)
Chin. Phys. B, 2026, 35 (**2**): 024210. DOI: 10.1088/1674-1056/ae1952

Temperature and acoustic impedance simultaneous sensor based on forward stimulated Brillouin scattering in highly nonlinear fiber

Shilong Liu(刘仕龙), Yang Li(李阳), Hongbin Hu(胡洪彬), Bing Sun(孙兵), and Zuxing Zhang(张祖兴)
Chin. Phys. B, 2025, 34 (**7**): 074212. DOI: 10.1088/1674-1056/adca1b

Engineering the spectra of photon triplets generated from micro/nanofiber

Chuan Qu(瞿川), Dongqin Guo(郭东琴), Xiaoxiao Li(李笑笑), Zhenqi Liu(刘振旗), Yi Zhao(赵义), Shenghai Zhang(张胜海), and Zhengtong Wei(卫正统)
Chin. Phys. B, 2024, 33 (**3**): 034208. DOI: 10.1088/1674-1056/ad1c5d

Generation of spectrally uncorrelated biphotons via fiber nonlinear quantum interference

Zhengtong Wei(卫正统), Chuan Qu(瞿川), Tian'an Wu(吴天安), Yuanyuan Li(李媛媛), Bo Li(李博), and Shenghai Zhang(张胜海)
Chin. Phys. B, 2023, 32 (**6**): 064202. DOI: 10.1088/1674-1056/acb767

Cascaded optical frequency transfer over 500-km fiber link using regenerative amplifier

Xue Deng(邓雪), Dong-Dong Jiao(焦东东), Jie Liu(刘杰), Qi Zang(臧琦), Xiang Zhang(张翔), Dan Wang(王丹), Jing Gao(高静), Rui-Fang Dong(董瑞芳), Tao Liu(刘涛), Shou-Gang Zhang(张首刚)
Chin. Phys. B, 2020, 29 (**5**): 054205. DOI: 10.1088/1674-1056/ab7b4f

---

A high-gain optical injection amplification system for coherent fiber links

Ru Yuan(袁茹)[1,2,3], Xiang Zhang(张翔)[1,3,†], Qian Zhou(周茜)[1,3], Qi Zang(臧琦)[1,3], Lin-Bo Zhang(张林波)[1,3], Yi-Ting Liu(刘依婷)[1,3], Dan Wang(王丹)[1,3], Jie Liu(刘杰)[1,3], Yu-Can Zhang(张钰灿)[1,3], Yu-Fang Lei(雷语芳)[1,3], Tao Liu(刘涛)[1,2,3,‡], Rui-Fang Dong(董瑞芳)[1,2,3,§], and Shou-Gang Zhang(张首刚)[1,2,3,¶]

[1] *National Time Service Center, Xi'an* 710600, *China*
[2] *University of Chinese Academy of Sciences, Beijing* 100049, *China*
[3] *Key Laboratory of Time and Frequency Standards, Chinese Academy of Sciences, Xi'an* 710600, *China*

(Received 7 August 2025; revised manuscript received 23 September 2025; accepted manuscript online 9 October 2025)

We design a high-gain optical amplification system based on optical injection locking (OIL) technology, which has an all-fiber structure and is ideally suited for fiber-based optical frequency transfer system. The paper investigates the relationship between amplification gain and frequency detuning under different injection linewidths, showing that smaller injection linewidths result in higher gains for the same frequency detuning. Preliminary experiments show that with a 5 Hz injection linewidth and sufficiently small frequency detuning, an amplification gain exceeding 60 dB can be achieved. In contrast to previous approaches, we introduce an out-of-loop optical path with an acousto-optic modulator to counteract the additional phase noise introduced by the asymmetric optical paths, achieving a higher-performance optical injection amplification system. After effective phase noise suppression, the noise floor of 1m coherent fiber link constructed based on the optical amplification system achieves a fractional frequency instability floor of 1.6×10^{-20} at an integration time of 10000 s. Based on this high-performance system, a long-distance coherent transmission experiment over a 200 km spooled fiber link was demonstrated, which showed a fractional frequency instability of 3.4×10^{-15} at 1 s, scaling down to 3.4×10^{-20} at 10000 s in terms of modified Allan deviation (Mod-ADEV). This work presents a high-gain optical amplification method for transferring ultra-stable optical frequency standards, reducing the number of repeaters and amplifiers in optical frequency transfer, and simplifying the system complexity.

Keywords: optical injection amplifier, optical frequency transfer, coherent fiber link, phase noise cancellation

PACS: 42.81.–i, 06.30.Ft, 95.55.Sh

DOI: 10.1088/1674-1056/ae111a **CSTR:** 32038.14.CPB.ae111a

1. Introduction

The instability and uncertainty of optical clock system in the world have now reached the 10^{-18} level,[1–4] and the clock network linking these high-precision optical frequency standards will greatly promote the development of radio astronomy,[5] seismology,[6] gravitational wave, dark matter detection[7,8] and frequency metrology.[9] Among various frequency transfer and comparison methods, traditional satellite-based technical solutions cannot be applied due to limited transmission accuracy,[10] while the fiber-optic links have proven to be highly effective for distributing and comparing state-of-the-art optical clocks due to their characteristics of low attenuation, anti-interference and large bandwidth.[11,12]

To achieve high-performance of the fiber-based optical frequency transfer, it is essential to compensate for the power attenuation that occurs during long-distance transmission. Consequently, various amplification techniques are employed to compensate optical attenuation and increase the transmission distance. The bi-directional erbium-doped fiber amplifier (Bi-EDFA) has been extensively utilized for the coherent fiber links due to its straightforward design and efficient operation. However, its effective gain in practical application is commonly limited to less than 20 dB due to the presence of the lasing effect caused mainly by end-face reflections and Rayleigh scattering.[13] Additionally, the unwanted amplified spontaneous emission (ASE) noise generated during the amplification process will degrade the optical signal-to-noise ratio (OSNR) and deteriorate the transfer performance. In 2010, the fiber Brillouin amplification (FBA) with transfer fiber link as the gain medium was proposed and demonstrated as an alternative and effective amplifier solution, which provided a narrow amplification bandwidth of 20 MHz and a higher gain of 50 dB.[14] In this configuration, the phase of the pump laser should be locked to the transmitted light with the offset Brillouin frequency of about 11 GHz.[15,16] Despite its excellent performance, this system is unable to eliminate the intensity noise inherent in the transmitted optical signal and necessi-

†Corresponding author. E-mail: zhangxiang@ntsc.ac.cn
‡Corresponding author. E-mail: taoliu@ntsc.ac.cn
§Corresponding author. E-mail: dongruifang@ntsc.ac.cn
¶Corresponding author. E-mail: szhang@ntsc.ac.cn

© 2026 Chinese Physical Society and IOP Publishing Ltd. All rights, including for text and data mining, AI training, and similar technologies, are reserved.

tates a strong pump laser. This requirement may introduce additional stray laser light within the coherent link, subsequently reducing the OSNR of the high-precision optical signal. Furthermore, the same solutions utilizing EDFA[17] and Raman amplification[18] are also ineffective in addressing these issues.

To address the issue, Kim *et al.* proposed and investigated optical injection amplification as a mid-stage amplifier to achieve high optical gain in establishing a coherent fiber link, a single-span 146 km installed fiber link with transfer instability below 10^{-19} was achieved.[19] In order to further optimize the system structure to reduce the additional phase noise, Feng *et al.* studied the optical injection amplifier with an acousto-optic modulator (AOM) based coherent detection scheme,[20,21] in which the phase noise for different injection ratios corresponding to transfer frequency instability was investigated. Their work also examined the relationship between the amplification gain and the frequency detuning between the master and slave lasers. However, above-mentioned studies did not consider the relationship between the linewidth of the injected light and the achieved amplification gain. As the linewidth of a narrow-linewidth laser broadens when passing through optical fibers of varying lengths, the required minimum injection power for the injected light changes as the linewidth increases, leading to variations in amplification gains.

In this paper, we construct a high-gain OIL-based amplification system and investigate the impact of key core parameters related to the injection conditions, including the injection linewidth, the injected optical power, and the frequency detuning, on the ultimate achievable optical gain of the amplification system. An external AOM was incorporated to realize noise detection and suppression, resulting in low additional phase noise in the optical amplification system. Consequently, the coherent optical frequency transmission system utilizing this system achieved a noise floor on the order of 10^{-20}. Finally, we experimentally validate this approach by transferring optical frequency over a 200 km spooled fiber link, achieving the fractional frequency instability of 3.4×10^{-15} at integration time of 1 s and 3.4×10^{-20} at 10000 s. The experimental results demonstrate that the OIL-based amplification system is well-suited for establishing coherent fiber link for the transmission and comparison of state-of-the-art optical clock signals.

2. Experimental setup

The phenomenon of optical injection locking occurs when light from a master laser is injected into a slave laser, enabling the slave laser to surpass its internal spontaneous emission. Consequently, the output of the slave laser tracks the frequency of the master laser while maintaining a fixed phase offset, which is determined by the frequency detuning between the two lasers. Figure 1 depicts the principle diagram of OIL-based optical amplification. The slave laser is a semiconductor laser without an optical isolator in this case, and upon successful injection, its frequency will track that of the master laser, resulting in an output power equivalent to that of the master laser. Since the power of the input signal is usually much lower than that of the slave laser, the OIL-based system effectively functions as an amplifier for the input signal.

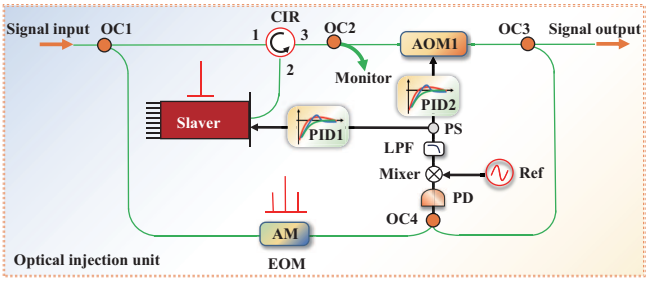


Fig. 1. The high-gain OIL-based optical amplification system based optical injection locking. AOM, acousto-optic modulator; AM, amplitude modulator; EOM, electro-optic modulator; CIR, circulator; PD, photodetector; LPF, low pass filter; PS, power splitter; PID, proportional-integral-derivative; Ref, reference; Monitor, laser wavelength monitoring.

2.1. Principle of OIL based amplifier system

As illustrated in Fig. 1, the input light (master laser) with a frequency of ω_{m} which has passed through an optical fiber and is split into two parts. A small portion of the light passes through the electro-optical modulator (EOM) working at amplitude modulation (AM) mode, while the remaining portion is injected into the slave laser through the port 1 of optical circulator. Once the injection lock is completed, the laser frequency exiting from port 3 is equal to that of the master laser, and the output power is the same as that of the slave laser. A wavelength meter (High-Finesse, WS-7) is used in the experiment to confirm the success of the injection. The amplified light then passes through an AOM with a frequency shift of 30 MHz. The slave laser selected in this study is a distributed feedback (DFB) laser with a central wavelength of approximately 1550.12 nm and a linewidth of 2 kHz, which is operated using a commercial driver (Thorlabs, CLD1015). Its operating temperature ranges from 25 °C to 35 °C, and the driving current does not exceed 100 mA. The injection process introduces additional phase noise, at the same time, the slave laser exhibits slow drift.

To achieve long-term stability in the optical injection system, the two signals entering the photodetector (PD) carry the frequency (phase) fluctuation information introduced during the injection process and the AM sidebands noise. The error signal is divided into two paths: one feeds back to the slave laser for locking, while the other suppresses the phase noise introduced by the injection process. The use of the AM enables the system to detect phase variations with higher sensitivity, thereby facilitating ultra-high-precision feedback control. It should be emphasized that the enhanced locking capability of

the system is achieved through the joint application of the AM, AOM and the phase-locked loop (PLL).

Using the basic theoretical model of injection locking,[22,23] the achieved gain G_0 by the OIL based amplification system can be expressed as

$$G_0 = \gamma^{-1} = \left(\frac{A_m}{A_s}\right)^{-1} = \left(\frac{-\Delta\omega}{\kappa\sqrt{1+\alpha^2}\sin(\varphi_L + \tan^{-1}\alpha)}\right)^{-1}, \quad (1)$$

the optical injection ratio γ represents the ratio of the injection light power A_m to the slave laser power A_s, the $\Delta\omega$ and φ_L respectively represent the frequency detuning and phase difference between the master laser and slave laser. The κ is the coupling coefficient and α is the linewidth enhancement factor. Successful injection locking can be achieved as long as the detuning frequency $\Delta\omega$ is smaller than the locking bandwidth ω_{LB}, which are given by following expression:

$$\omega_{LB} = \Delta\omega_{max} - \Delta\omega_{min}, \quad (2)$$

$$-\kappa\sqrt{1+\alpha^2}\frac{A_m}{A_s} = \Delta\omega_{min} < \Delta\omega < \Delta\omega_{max} = \kappa\frac{A_m}{A_s}, \quad (3)$$

the parameter α quantifies the phase shift in the slave laser due to refractive index variations caused by changes in carrier density. Since α is non-zero, it introduces asymmetry in the locking range, and the achieved gain G_0 exhibits asymmetry in both positive and negative frequency detuning. Therefore, during injection locking adjustment, it is common to approach the frequency of the slave laser's frequency from the negative frequency direction. From the established model, it can be seen that in order to obtain a high gain, we need to reduce $\Delta\omega$ as much as possible.

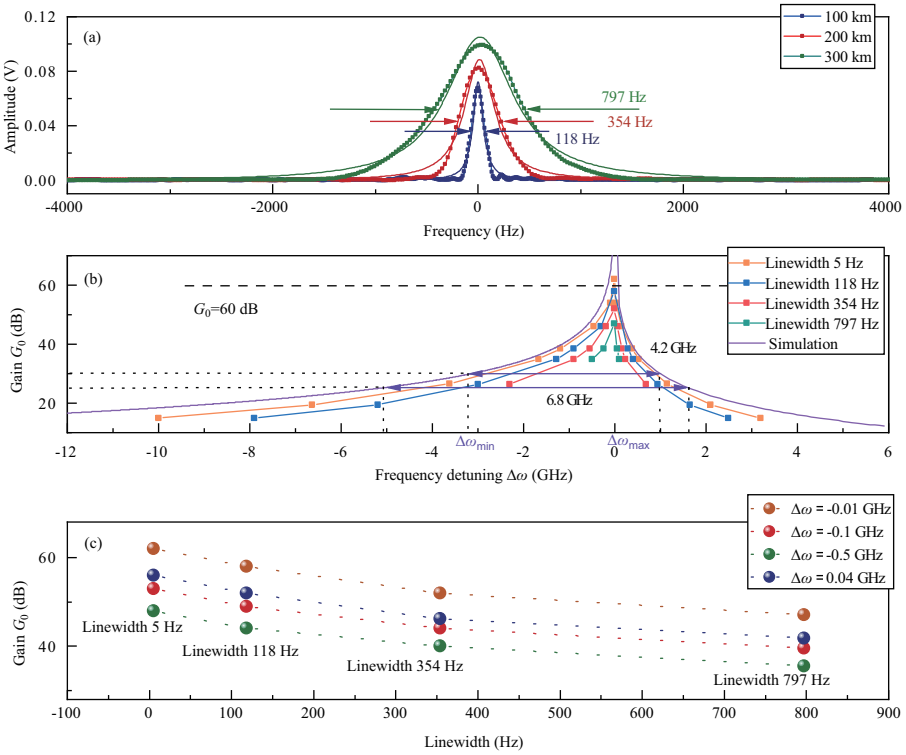


Fig. 2. (a) Measurement of the laser linewidth broadening of narrow-linewidth laser after passing through fibers of varying lengths. (b) The relationship between the achieved gain G_0 and frequency detuning $\Delta\omega$ for different injection laser linewidths. The purple curve represents the simulation result. (c) Graph showing the relationship between the achieved gain G_0 and linewidth at different frequency detuning values.

In addition, we explored the relationship between G_0 and the linewidth ν_m of the injected master laser. An ultra-stable laser with a 5 Hz initial linewidth was used in conjunction with optical fibers of various lengths to generate the master laser with different linewidths. As shown in Fig. 2(a), the linewidths were measured using the beat frequency method followed by Lorentzian fitting. The results indicate that as the transfer distance increases, the linewidth of the injected light broadens. When the fiber length reaches 300 km, the linewidth increases to approximately 797 Hz. Based on the obtained four groups of injected light with different linewidths, we investigated the relationship between gain G_0 and frequency detuning $\Delta\omega$, the results are illustrated in Fig. 2(b), the purple simulation curve and the other three experimental data curves demonstrate that the relationship between G_0 and frequency detuning is asymmetric about zero, with the experimental results closely matching with the simulation. We experimentally determined the minimum injection power by gradually reducing the injection power while observing whether the system could maintain continuous and stable locking. It is worth noting that with an injection light linewidth of 5 Hz and a minimum frequency detuning of −0.01 GHz (limited to a mea-

surable minimum of 10 MHz by the wavelength meter's accuracy), the minimum injection power can be as low as −52 dBm (approximately 6.31 μW), while the output power is equal to that of the slave laser (10.7 dBm), resulting in a corresponding gain of 62.7 dB. Additionally, the data in Fig. 2(c) show that a smaller injection linewidth corresponds to a higher gain, and a larger locking bandwidth, which aligns well with the requirements of our application. The minimum injection power under different linewidths has been summarized in Table 1.

Table 1. The minimum injection power and output power.

Linewidth (Hz)	Input (dBm)	Onput (dBm)	Gain (dB)	$\Delta\omega$ (GHz)
5	−52.0	10.7	62.7	−0.01
118	−47.3	10.7	58.0	−0.01
354	−41.9	10.7	52.6	−0.01
797	−36.3	10.7	47.0	−0.01

2.2. The Coherent fiber link established by using OIL based amplifier system

In the injection locking module (Fig. 1), we utilize acousto-optic modulators (AOM) to suppress phase noise during the locking process, along with an amplitude modulator (AM). The amplitude modulator extends the locking range and improves stability, ensuring robust locking even when the detuning ($\Delta\omega$) is large and the slave laser (distributed feedback laser, DFB) drifts slowly with time.

In this optical system, asymmetric optical paths can significantly impact system performance, particularly in terms of phase and frequency stability. Since the circulator is unidirectional, some degree of asymmetry in the system is inevitable. Therefore, it is essential to minimize the influence of these asymmetric optical paths. One of the main objectives of this paper is to mitigate the effects of asymmetry on the optical injection locking system. To address this, we design an external optical path where a portion of the output light is split off, reflected by the partial Faraday mirror (PFM), passes through the AOM, and then returns to the local path. The returned light is subsequently mixed with the local light for beat frequency detection, thereby compensating for the impact of the asymmetric optical path.

The detailed experimental setup of the optical frequency transmission system based on optical injection locking, combined with bidirectional comparison technology, is shown in Fig. 3. The master laser used in the system is a commercially available narrow-linewidth laser with a linewidth of 5 Hz. Similar to conventional optical frequency transfer systems, the system consists of three parts: the local site, the measurement section, and the remote end.

At the local site, light from the master laser is split using an X-type splitter OC1. A small portion of this light passes through AOM3 (down-shifted mode, 160 MHz) and reaches PD3, where it is reflected back to point A for bidirectional comparison. Another portion is reflected by PFM1 to photodetector PD1 as a reference signal. The majority of the light passes through AOM1, which operates in down-shifted mode with a driving frequency of 157 MHz at the local site and is transmitted to remote site via optical fiber and port 2 of the circulator. The AOM1 is primarily employed to suppress phase noise of the fiber optic links.

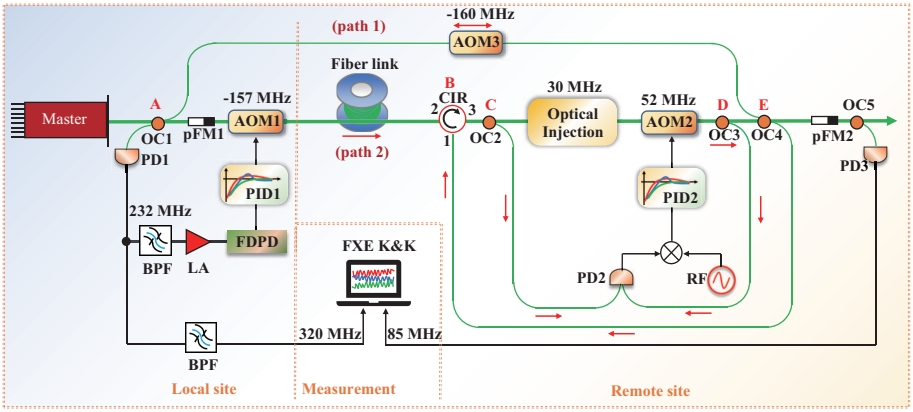


Fig. 3. Schematic diagram of the optical frequency transfer system based on optical injection locking amplification. Laser, narrow linewidth laser; PFM, partial Faraday mirror; AOM, acousto-optic modulator; AM, amplitude modulator; PD, photodetector; FDPD: a programmable digital frequency division phase discriminator; BPF, band-pass filter; LA, logarithmic amplifier; PID, proportional-integral-derivative.

After transmission to the remote site, the light is split into two parts, one part is injected to the optical injection system, while the other is used for beat frequency detection with the light from AOM2 driven with a frequency of 52 MHz in the second loop. This helps eliminate the phase noise induced by the asymmetric optical path of the optical injection part, ensuring phase alignment of points C and D. The light from AOM2 is split, with one portion entering PD2 for beat frequency measurement and the other portion returning to the local site via a circulator. The circulator is primarily used to return the amplified light to the local site for comparison and to transmit the light to the optical injection part. Under the ideal condition, the phase noise of the loop can be perfectly compensated by suppressing the phase noise detected by PD1. The beating sig-

nal of 232 MHz between the round trip and the reference carries the phase information of the fiber link and the asymmetric path. The 320 MHz signal detected by PD1 is generated through the beat frequency between the master laser ν_0 and the light that double-passed path 1 and returned to PD1. The phase information carried by this 320 MHz signal is denoted as $2\varphi_3$. To minimize nonlinear effects in the fiber and achieve a high-performance optical frequency transfer system, it is crucial to reduce any additional phase contributions. The AOM3 plays an important role in mitigating the phase noise caused by the asymmetric optical path, the signal detected by PD3 is obtained from the light in path 2 $(\nu_0 - 157 + 30 + 52)$ MHz and the light in path 1 $(\nu_0 - 160)$ MHz, resulting in an 85 MHz signal carrying phase information $(\varphi_1 - \varphi_3)$. In the measurement section, the 160 MHz signal, obtained by dividing the 320 MHz signal by a factor of 2, carries phase information φ_3. When the 160 MHz signal is mixed with the 85 MHz signal, the resulting 245 MHz signal carries phase information φ_1, which corresponds to the phase information of the output light. This process effectively eliminates the influence introduced by the AOM3 measurement path.[24]

Due to the use of an optical circulator, asymmetrical optical paths are inevitably present in the experiment. Since the optical fibers used are made of the same material and have identical thermal sensitivity coefficients, the asymmetric equivalent length of the fiber segments BC, DE, and BE (shown in Fig. 3) can be expressed as[25]

$$L_{\mathrm{e}} = L_{\mathrm{BC}} + L_{\mathrm{DE}} - L_{\mathrm{BE}} \tag{4}$$

to achieve a high-performance optical frequency transfer system, it is essential to minimize any additional phase contributions. We minimized the lengths of the fiber segments BC, DE and BE, while ensuring that asymmetric equivalent length L_{e} is as close to zero as possible. To verify the suitability of the amplifier for the establishment of coherent fiber optic links, we constructed an optical frequency transfer system based on it, measured the system's noise floor, furthermore, experiments were conducted with a single-span distance of 200 km, for which the total fiber loss was measured to be 44 dB. The transmission performance was then tested and analyzed in both time and frequency domains. To characterize system properties such as fractional frequency stability and phase noise PSD, we employed a dead-time free frequency counter (FXE K&K) and a commercial noise analyzer (Rohde&Schwarz, FSWP).

3. Experimental results

Figure 4 presents the measurement results of the system's noise floor. In this scenario, an adjustable optical fiber attenuator approximately 20 cm in length was employed to connect the local and remote ends, following the methods described in the literature.[26] In the frequency domain, the phase noise PSDs in both free-running (dark blue curve) and stabilized (red curve) conditions were measured, as shown in Fig. 4(a). In the free-running case, the phase noise PSD exhibits a decline proportional to f^{-3} in the Fourier frequency range from 1 Hz to 10 Hz , and f^{-2} linearity from 10 Hz to 100 Hz. After compensation, the phase noise PSD follows a power law of f^0 from 10 Hz to 100 Hz, achieving a noise suppression ratio of approximately 37.9 dB at a Fourier frequency of 1 Hz. The fractional frequency instability, a key time-domain characteristic, is calculated using the recorded frequency values and is shown in Fig. 4(b), representing the system's noise floor under stabilized condition. No cycle slips were observed throughout the entire frequency measurement period. In the stabilized case, the fractional frequency instability is 5.6×10^{-17} for an integration time of 1 s, and scales down to 1.6×10^{-20} at 10000 s in terms of Mod-ADEV (red circles). These results demonstrate that the OIL-based amplification system exhibits exceptional performance and is well-suited for establishing a coherent fiber link for the transmission and comparison of state-of-the-art optical clock signals.

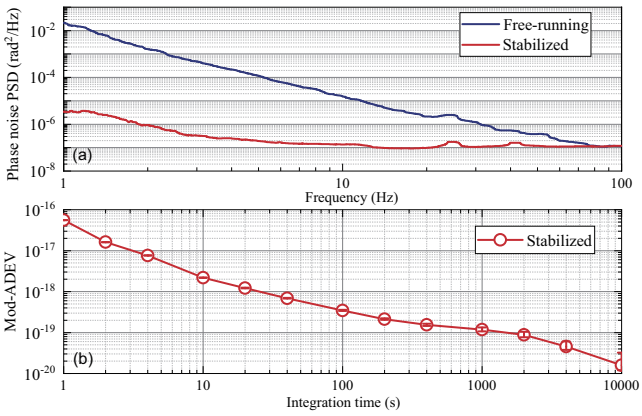


Fig. 4. The measurement results of the system's noise floor are as follows. (a) The phase noise power spectral densities (PSDs) measured under free-running conditions (dark blue curve) and stabilized conditions (red curve) using the shortcut method. (b) The fractional frequency instability of the transfer system under stabilized conditions, measured with a Π-type frequency counter and represented by Mod-ADEV (red circles).

Furthermore, we conducted laboratory experiments to evaluate the properties of the 200 km coherent spooled fiber link. The measured phase noise PSD is illustrated in Fig. 5(a), the phase noise PSD in the unsuppressed case S_{free} (blue curve) follows the relationship of h_0/f^2 with Fourier frequency f, indicating that white frequency noise predominantly contributes to the characteristics of the fiber link when no noise suppression is applied. After implementing a noise compensation, the residual phase noise PSD $S_{\mathrm{r}}(f)$ (red curve), follows a different dependence on the Fourier frequency with $h_1 f^0$, demonstrating that the residual phase noise is primarily dominated by white phase noise in the stabilized condition. The theoretical

suppression limitation for phase noise PSD $S_t(f)$ can be derived using the following time delay τ correlation formula[27]

$$S_t = \frac{1}{3}(2\pi f\tau)^2 S_{free}, \tag{5}$$

where $\tau = nL/c$, $n = 1.468$ is the refractive index of the fiber, L is the fiber length, and c is the speed of light in a vacuum. The theoretical result (green curve) aligns closely with the measured residual phase noise, confirming the effectiveness of the noise suppression technique. Notably, the phase noise PSD in the free-running condition aligns with that in the stabilized case at the Fourier frequency $1/4\tau$. The suppression bandwidth of the 200 km fiber link was measured to approximately 250 Hz, which is consistent with theoretical predictions.

After studying the frequency-domain characteristics, the time-domain feature of the fractional frequency instability of the 200 km coherent fiber link was analyzed and shown in Fig. 5(b). Prior to noise suppression, the frequency instability (blue triangle) reaches 5.5×10^{-13} at 1 s integration time, fluctuating around the 10^{-14} level. After implementing noise suppression, the frequency instability improved to approximately 3.4×10^{-15} at 1 s and further decreased to 3.6×10^{-19} at 10000 s, with a slope of τ^{-1} in terms of the overlapping Allan deviation (OADEV). In Mod-ADEV mode, the fractional frequency instability decreases to 3.4×10^{-20} with a slope of $\tau^{-3/2}$ at 10000 s, indicating that white noise dominates the system, consistent with the results shown in Fig. 5(a).

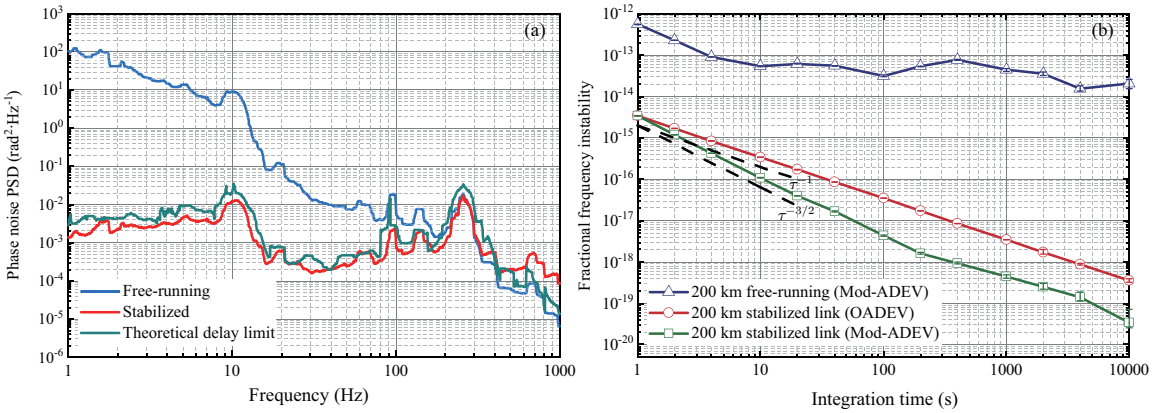


Fig. 5. (a) The measured phase noise PSDs of the 200 km coherent fiber link respectively in the free-running case (dark blue curve) and the stabilized case (red curve). The theoretical compensation limitation due to time delay is also indicated (green dashed line). (b) The measured fractional frequency instabilities in the free-running case (dark blue triangles) and the stabilized case, represented in terms of OADEV (red circles) and Mod-ADEV (green squares), using a Π-type frequency counter. Error bars are included within the symbols.

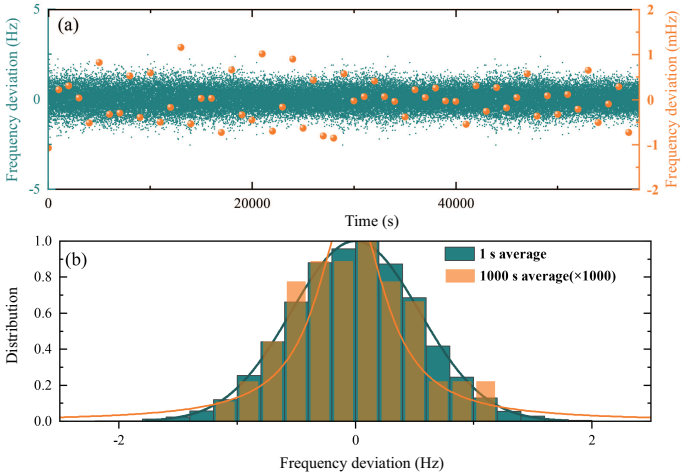


Fig. 6. (a) Frequency data collected using a dead-time-free PI-mode frequency counter with a 1-second counting time, resulting in 58000 data points (dark cyan, left axis). The unweighted arithmetic means of these data points are represented by 58 mean values (orange, right axis). (b) Histograms and Gaussian fits for the recorded frequency values (dark cyan dots) and the 58 arithmetic mean values (orange dots), illustrating the distributions and statistical characteristics of the data.

In addition, we conducted an accuracy evaluation of the frequency data following optical injection locking amplification over a stabilized 200 km fiber link with total loss of 44 dB. Figure 6(a) illustrates the frequency deviation of the transmitted signal after noise suppression. The data were recorded using a Π-type mode with a 1-second gate time, a total of 58000 data points (illustrated as dark cyan dots on the left axis) were measured and evenly divided into 58 groups of 1000 data points each, yielding 58 averaged values. Figure 6(b) presents the histogram and Gaussian fit for the recorded frequency values, along with the 58 averaged points. The arithmetic mean of the obtained data is 29.8 Hz (1.5×10^{-19}), with a standard deviation of 0.49 mHz (2.5×10^{-18}). Taking into account the results of Fig. 5, we conservatively estimate that the systematic uncertainty is smaller than 3.2×10^{-19}. Within this uncertainty range, the retrieved light at the remote site shows no frequency deviation relative to the local reference light. These above-mentioned results demonstrate that the OIL-based amplification system is highly effective for transmitting advanced optical clock signals, making it ideal for state-of-the-art frequency metrology applications.

4. Conclusion

In this study, we focus on the development of a substantial optical amplification system using an OIL technology. Initially, we design a high-gain OIL-based amplification system capable of delivering ultra-precision optical frequency signals. The effects of injection linewidth, frequency detuning and injection power on the achievable optical gain of the OIL-based amplifier are systematically investigated. Experimental results demonstrate that the system can achieve an amplification exceeding 60 dB, significantly extending the transfer distance between sites. To mitigate the residual phase noise introduced by the asymmetric optical paths, an AOM was incorporated to facilitate noise detection and suppression. Based on this OIL-based amplifier, the coherent frequency transfer system has a noise floor of 10^{-20} level. This low noise floor ensures reliable transfer of optical frequency signals over longer distances. Additionally, we demonstrate the system performance over 200 km coherent spooled fiber link, achieving an instability of 3.4×10^{-20} at 10000 s. These findings indicate that optical injection locking is a promising approach for long-distance optical frequency transfer, offering a robust solution for reducing system complexity.

Acknowledgments

Project supported by the National Major Science and Technology Infrastructure Project of China, for "High Precision Ground-based Time Service System" (Grant No. 2017-000052-73-01-00240), the National Natural Science Foundation of China (Grant No. 12303077), and the Innovation Program for Quantum Science and Technology (Grant No. 2021ZD0300900).

References

[1] Riehle F 2017 *Nat. Photon.* **11** 25
[2] Oelker E, Hutson R B, Kennedy C J, Sonderhouse L, Bothwell T, Goban A, Kedar D, Sanner C, Robinson J M, Marti G E, Matei D G, Legero T, Giunta M, Holzwarth R, Riehle F, Sterr U and Ye J 2019 *Nat. Photon.* **13** 714
[3] Li J, Cui X Y, Jia Z P, Kong D Q, Yu H W, Zhu X Q, Liu X Y, Wang D Z, Zhang X, Huang X Y, Zhu M Y, Yang Y M, Hu Y, Liu X P, Zhai X M, Liu P, Jiang X, Xu P, Dai H N, Chen Y A and Pan J W 2024 *Metrologia* **61** 015006
[4] Lu X T, Guo F, Liu Y Y, Cao J, Li J A, Xia J J, Xu Q F, Lu B Q, Wang Y B and Chang H 2025 *Metrologia* **62** 035007
[5] Pizzocaro M, Sekido M, Takefuji K, *et al.* 2020 *Nat. Phys.* **17** 223
[6] Marra G, Fairweather D M, Kamalov V, Gaynor P, Cantono M, Mulholland S, Baptie B, Castellanos J C, Vagenas G, Gaudron J O, Kronjager J, Hill I R, Schioppo M, Edreira I B, Burrows K A, Clivati C, Calonico D and Curtis A 2022 *Science* **376** 874
[7] Kolkowitz S, Pikovski I, Langellier N, Lukin M D, Walsworth R L and Ye J 2016 *Phys. Rev. D* **94** 124043
[8] Roberts B M, Delva P, Al-Masoudi A, *et al.* 2020 *New J. Phys.* **22** 093010
[9] Chanteau B, Lopez O, Zhang W, Nicolodi D, Argence B, Auguste F, Abgrall M, Chardonnet C, Santarelli G, Darquie B, Le Coq Y and Amy Klein A 2013 *New J. Phys.* **15** 073003
[10] Petit G, Kanj A, Loyer S, Delporte J, Mercier F and Perosanz F 2015 *Metrologia* **52** 301
[11] Predehl K, Grosche G, Raupach S M, Droste S, Terra O, Alnis J, Legero T, Hansch T W, Udem T, Holzwarth R and Schnatz H 2012 *Science* **336** 441
[12] Lindvall T, Pizzocaro M, Godun R M, *et al.* 2025 *Optica* **12** 843
[13] Chiodo N, Quintin N, Stefani F, Wiotte F, Camisard E, Chardonnet C, Santarelli G, Amy-Klein A, Pottie P E and Lopez O 2015 *Opt. Express* **23** 33927
[14] Terra O, Grosche G and Schnatz H 2010 *Opt. Express* **18** 16102
[15] Raupach S M F, Koczwara A and Grosche G 2014 *Opt. Express* **22** 26537
[16] Kadum J E, Ji J, Kuhl A, Misera M, Waterholter T and Koke S 2023 *APL Photonics* **8** 036113
[17] Terra O, Grosche G, Predehl K, Holzwarth R, Legero T, Sterr U, Lipphardt B and Schnatz H 2009 *Appl. Phys. B* **97** 541
[18] Clivati C, Bolognini G, Calonico D, Faralli S, Levi F, Mura A and Poli N 2013 *IEEE Photon. Technol. Lett.* **25** 1711
[19] Kim J, Schnatz H, Wu D S, Marra G, Richardson D J and Slavik R 2015 *Opt. Lett.* **40** 4198
[20] Feng Z, Yang F, Zhang X, Chen D, Wei F, Cheng N, Sun Y, Gui Y and Cai H 2018 *Sci. Rep.* **8** 13135
[21] Feng Z, Zhang X, Wu R, Sun Y, Wei F, Yang F, Gui Y and Cai H 2019 *IEEE Photonics J.* **11** 1
[22] Liu Z and Slavik R 2019 *J. Lightwave Technol.* **38** 43
[23] Skehan J C, Karlsson M and Andrekson P A 2024 *Opt. Express* **32** 1956
[24] Xue R, Hu L, Shen J, Chen J and Wu G, 2021 *J. Lightwave Technol.* **39** 4638
[25] Zhou Q, Zhang X, Zang Q, Wu M, Wang D, Liu J, Dong R, Liu T and Zhang S 2024 *Chin. Phys. Lett.* **41** 084202
[26] Hu L, Tian X, Wu G, Kong M, Shen J and Chen J 2020 *J. Lightwave Technol.* **38** 3644
[27] Williams P A, Swann W C and Newbury N R 2008 *J. Opt. Soc. Am. B* **25** 1284